(12) INTERNATIONAL APPLICATION PUBLISHED UNDER THE PATENT COOPERATION TREATY (PCT)

(19) World Intellectual Property Organization

International Bureau



### 

(10) International Publication Number WO 2012/100038 A2

(43) International Publication Date 26 July 2012 (26.07.2012)

(21) International Application Number:

PCT/US2012/021847

(22) International Filing Date:

19 January 2012 (19.01.2012)

(25) Filing Language:

English

(26) Publication Language:

English

(30) Priority Data:

61/434,071 19 January 2011 (19.01.2011) US

(71) Applicants (for all designated States except US): THE RESEARCH FOUNDATION OF STATE UNIVERSITY OF NEW YORK [US/US]; University at Buffalo, Office of Science, TechnoLogy Transfer and Economic Outreach, Baird Research Part, Suite 111, 1576 Sweet Home Road, Amherst, NY 14228 (US). U.S ARMY RESEARCH LABORATORY [US/US]; 2800 Powder Mill Road, Adelphi, MD 20783-1197 (US).

(72) Inventors; and

(75) Inventors/Applicants (for US only): MITIN, Vladimir [US/US]; 1860 North Forest Road, Amherst, NY 14221 (US). SERGEYEV, Andrei [US/US]; 41 Oak Street, Apt. #1, Amherst, NY 14228 (US). VAGIDOV, Nizami [US/US]; 215 Palmdale Drive, Williamsville, NY 14221 (US). LITTLE, John, W. [US/US]; 4268 Knobs end Court, Ellicott City, MD 21042 (US). REINHARDT, Kitt

[US/US]; 9513 Milstead Drive, Bethesda, MD 20817 (US). **SABLON, Kimberly** [US/US]; 4960 Walking Stick Road, Apt. G, Ellicott City, MD 21043 (US).

- (74) Agents: WATT, Rachel, S. et al.; Hodgson Russ LLP, The Guaranty Building, 140 Pearl Street, Suite 100, Buffalo, NY 14202-4040 (US).
- (81) Designated States (unless otherwise indicated, for every kind of national protection available): AE, AG, AL, AM, AO, AT, AU, AZ, BA, BB, BG, BH, BR, BW, BY, BZ, CA, CH, CL, CN, CO, CR, CU, CZ, DE, DK, DM, DO, DZ, EC, EE, EG, ES, FI, GB, GD, GE, GH, GM, GT, HN, HR, HU, ID, IL, IN, IS, JP, KE, KG, KM, KN, KP, KR, KZ, LA, LC, LK, LR, LS, LT, LU, LY, MA, MD, ME, MG, MK, MN, MW, MX, MY, MZ, NA, NG, NI, NO, NZ, OM, PE, PG, PH, PL, PT, QA, RO, RS, RU, RW, SC, SD, SE, SG, SK, SL, SM, ST, SV, SY, TH, TJ, TM, TN, TT, TZ, UA, UG, US, UZ, VC, VN, ZA, ZM, ZW.
- (84) Designated States (unless otherwise indicated, for every kind of regional protection available): ARIPO (BW, GH, GM, KE, LR, LS, MW, MZ, NA, RW, SD, SL, SZ, TZ, UG, ZM, ZW), Eurasian (AM, AZ, BY, KG, KZ, MD, RU, TJ, TM), European (AL, AT, BE, BG, CH, CY, CZ, DE, DK, EE, ES, FI, FR, GB, GR, HR, HU, IE, IS, IT, LT, LU, LV, MC, MK, MT, NL, NO, PL, PT, RO, RS, SE, SI, SK, SM, TR), OAPI (BF, BJ, CF, CG, CI, CM, GA, GN, GQ, GW, ML, MR, NE, SN, TD, TG).

[Continued on next page]

(54) Title: PHOTOVOLTAIC CELLS WITH QUANTUM DOTS WITH BUILT-IN-CHARGE AND METHODS OF MAKING SAME

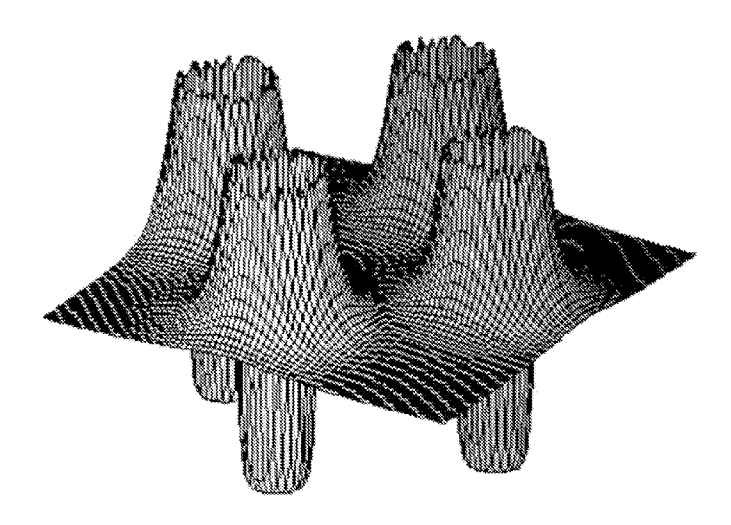


Figure 4

(57) Abstract: Devices (e.g., photovoltaic devices) with quantum dots with built-in charge and methods of making such devices. The quantum dots are in a layer of n-doped semiconductor material. The devices can exhibit improved conversion and electrical properties as compared to devices without such quantum dots and n-doping.



## WO 2012/100038 A2

#### Published:

without international search report and to be republished upon receipt of that report (Rule 48.2(g))

# PHOTOVOLTAIC CELLS WITH QUANTUM DOTS WITH BUILT-IN CHARGE AND METHODS OF MAKING SAME

#### CROSS-REFERENCE TO RELATED APPLICATIONS

5 **[0001]** This application claims priority to U.S. provisional patent application no. 61/434,071, filed January 19, 2011, the disclosure of which is incorporated herein by reference.

#### STATEMENT REGARDING FEDERALLY SPONSORED RESEARCH

[0002] This invention was made with government support under contract no.

W911NF-11-2-0079 awarded by the US Army Research Laboratory. The government has certain rights in the invention.

#### FIELD OF THE INVENTION

15

20

25

30

[0003] The present invention generally relates to devices with quantum dots. More particularly, the present invention relates to photovoltaic devices with quantum dots with built-in charge.

#### BACKGROUND OF THE INVENTION

[0004] Quantum dots (QD) are very promising candidates to create energy level structures for better use of the solar spectrum. In QDs the carriers are confined in all three dimensions with the allowed absorption bands being separated by the forbidden gaps. In such multiple energy level cells additional energy levels accommodate the mismatch between the solar spectrum and two-level electron transitions. In this way QD structures allow for minimizing so-called thermalization losses.

[0005] Quantum dot solar cells have been attractive for solar cell applications due to their ability to enhance light absorption via multiple energy levels introduced by quantum dots) and extend the absorption edge into the infrared range. Theoretical modeling of the intermediate band QD solar cell has predicted an increase in the efficiency up to approximately 64% for a well-adjusted intermediate band, but up to now the experimental work has shown very limited success. In contrast to the expected substantial increase in the photocurrent due to harvesting of infrared energy, the enhanced recombination of photocarriers via dots does not allow for a noticeable improvement of the short circuit current,  $J_{SC}$ . Moreover, in many cases even a small increase of  $J_{SC}$  was accompanied by the deterioration of the open circuit voltage,  $V_{OC}$ .

[0006] However, with increasing a number of possible photon induced transitions, QDs also enhance the inverse recombination processes and drastically increase the recombination losses. Despite the promising nature of QDs in solar technology there is a need for structures or arrangements that will substantially reduce these recombination losses.

[0007] The concept of QD solar cell is analogous to the concept of the impurity photovoltaic cell, which has been studied for many years. In the early sixties, Wolf proposed to use impurity levels to collect the long-wavelength radiation. In response, Shockley and Queisser argued that additional impurity levels drastically enhance the recombination processes (Shockley-Read-Hall recombination) and consequently deteriorate the device performance. Trade-off between IR energy harvesting and recombination losses due to impurity electron levels is a long-term problem studied without noticeable success in a number of theoretical and experimental investigations. However, compared to the midgap impurities, quantum dots offer more flexibility for nanoengineering of electron processes via dot size and selective doping.

#### 15 BRIEF SUMMARY OF THE INVENTION

5

10

20

[0008] The present invention provides devices (e.g., photovoltaic devices) with quantum dots with built-in charge (Q-BIC) and methods of making such devices. The dot charging is realized by n-doping the semiconductor material in which the dots are disposed. This approach provides control of a potential relief in the QD solar cell, and allows management of the photoelectron processes.

[0009] Use of charged quantum dots increases QD solar cell conversion efficiency. Without intending to be bound by any particular theory, it is considered the increased conversion is due to effective harvesting and conversion of IR radiation and suppression of recombination losses.

In an embodiment, the device comprises a plurality of quantum dots disposed in an n-doped semiconductor material, such that the quantum dots have built-in charge. The charge in the quantum dots creates potential barriers which prevent photoelectron capture by the quantum dots, and the electrons in the charged dots provide coupling to infrared radiation. The device is characterized by the built-in-dot charge of at least two electrons per dot. The device exhibits a short circuit current of at least 25 mA/cm<sup>2</sup>. The device is characterized by a lack of deterioration of open circuit voltage. The device does not have any intermediate quantum dot band.

[0011] In an embodiment, the device comprises a semiconductor substrate having disposed thereon a stack of layers. The stack of layers comprises a layer of n-doped or p-doped first semiconductor material, a layer of quantum dot medium comprising at least one layer of a second semiconductor material in which a plurality of quantum dots is disposed, where the layer is n-doped, and a layer of p-doped or n-doped third semiconductor material. If the first semiconductor material is n-doped the third layer of semiconductor material is p-doped, and if the first semiconductor material is p-doped the third layer of semiconductor material is n-doped at a level of at least two electrons per dot. In an embodiment, the stack of layers comprises a plurality of layers of semiconductor material in which a plurality of quantum dots is disposed.

[0012] In an embodiment, the method for making a device comprises the steps of providing a semiconductor substrate, depositing a layer of n-doped first semiconductor material or p-doped first semiconductor material on the substrate, fabricating a layer of quantum dot medium, and depositing a layer of n-doped semiconductor material, if p-doped material is the first layer deposited on the substrate, or p-doped semiconductor material, if n-doped material is the first layer deposited on the substrate.

[0013] The layer of quantum dot medium is fabricated by depositing a first layer of second semiconductor material, depositing a layer of quantum dot material, such that a plurality of quantum dots is formed, depositing a second layer of second semiconductor material and n-doping the layer, or depositing a second layer of second semiconductor material such that the second layer of second semiconductor material is n-doped. Optionally, these steps are repeated. In an embodiment, the second layer of second semiconductor material is deposited such that the n-dopants are in a discrete region of the second layer of second semiconductor material. The second layer of second semiconductor material is n-doped at a level of at least two electrons per dot.

#### BRIEF DESCRIPTION OF THE FIGURES

5

10

15

20

25

30

[0014] Figure 1. Losses in a solar cell: 1 - thermalization losses, 2 and 3 - losses related to junction and contact voltages, and 4 – recombination losses.

[0015] Figure 2. Schematic layout of a  $\delta$ -doped QD solar cell.

[0016] Figure 3. (a) Photogeneration of electron-hole pairs into the ground QD state  $(E_0)$  and into the excited QD state  $(E_1)$  followed by either thermionic emission  $(E_{therm})$  or intersubband photoexcitation  $(E_{isb})$  into the conducting channel;  $E_m$  is the direct photogeneration in the GaAs matrix. (b) Process induced by n-doping with IR transition of an

electron from the localized to the conducting state. (c) Another doping-induced process, where the radiation excites two electrons to QD excited states, then due to strong interelectron interaction in a QD one of these electrons transfers to the conducting state and the other transfers to a low-energy state.

- 5 [0017] Figure 4. Potential barriers around single dots in traditional QD structures with evenly distributed QDs.
  - [0018] Figure 5. *I-V* characteristics under 1 Sun (AM1.5 G) at 100 mW/cm<sup>2</sup> of QD solar cells as a function of doping: p-doped QD cell with 4 holes per dot, GaAs reference cell, undoped QD cell, n-doped QD cells with 2, 3, and 6 electrons per dot.
- 10 **[0019]** Figure 6. (a) Spectral response of GaAs reference and doped and undoped QD structures. (b) Magnified view of the spectral response in the range from 1000 to 1150 nm. (c) The spectral response of QD structure with 6 electrons per dot in the range 4000 8000 nm.
  - [0020] Figure 7. The long-wavelength photoresponse for undoped QD solar cell and n-doped cells with 2 and 6 electrons per dot under 1 Sun (AM1.5G) light passed through short-wavelength GaAs absorber.
  - [0021] Figure 8. Photoresponse to the 4300 nm IR radiation of a QD structure under the 620 nm optical pumping.
  - [0022] Figure 9. Room-temperature PL measurements at low excitation density for doped and undoped QD solar cells. (a) Dependence of the PL on the doping level for undoped device and n-doped devices with 2, 3, 4, and 6 electrons per dot and (b) comparison of PL in p-and n-doped devices with the same level of doping (4 carriers per dot).
  - [0023] Figure 10. (a) The three-dimensional (3D) potential profile of the conduction band in a QD solar cell. (Inset) Potential barriers around QD suppress the capture of photoelectrons. In the QD plane A-B, the potential between QDs varies from the maximum (D) to minimum (C). (b) Corresponding potential barriers for electrons in QD plane A-B as a function of built-in electron charge.

#### DETAILED DESCRIPTION OF THE INVENTION

15

20

25

30

- [0024] The present invention provides devices with quantum dots with built-in charge. These devices can be referred to as devices with quantum dots with built-in charge (i.e., Q-BIC devices). Also provided are methods of making such devices. For example, the devices are photovoltaic devices that can be used as solar cells.
- [0025] Two effects have been observed for the use of quantum dots with built-in charge in the present invention. First, it was observed the built-in charge enhances the IR-

induced intra-band transitions in quantum dots as well as transitions from the localized states in a dot to the conducting states in the semiconductor material matrix. Additionally, it was observed that this effect significantly increases electron coupling to IR radiation and improves harvesting of IR power in quantum dot solar cells (e.g., Fig. 3). Second, it was observed that the built-in charge creates potential barriers around quantum dots and these barriers exponentially suppress capture processes for photocarriers of the same sign as the built-in charge. Both effects radically improve the photovoltaic efficiency of quantum-dot solar cells (e.g., Fig. 4).

5

10

15

20

25

30

[0026] In an aspect, the present invention provides devices (e.g., photovoltaic devices) that have quantum dots with built-in charge. By "quantum dots with built-in charge" it is meant quantum dots disposed in a layer of semiconductor material that is n-doped. The amount of n-dopant is such that the quantum dots are at least partially filled by electrons from dopants, thus providing quantum dots with built-in charge. The devices with a Q-BIC medium can have long photoelectron lifetime and strong coupling to IR radiation due to the quantum dots with built-in charge.

[0027] In an embodiment, the device comprises a semiconductor substrate on which a stack of layers is disposed. The stack of layers comprises a layer of n-doped first semiconductor material, at least one layer of second n-doped semiconductor material in which a plurality of quantum dots is disposed, and a layer of p-doped third semiconductor material. The first semiconductor material, second semiconductor material, and third semiconductor material can be the same or different. The stack of layers is disposed on the substrate such that either the layer of n-doped semiconductor material or layer of p-doped semiconductor material is apposed to the substrate. In an embodiment, the device has a p-i-n junction with the QD medium embedded in the i-region.

[0028] The semiconductor substrate can be any of any semiconductor material on which the stack of layers can be formed. The substrate can have a range of sizes and shapes. Examples of suitable materials include, but are not limited to, GaAs, InP, Si, BaF<sub>2</sub>, CaF<sub>2</sub>, or SiC. An example of a substrate is a Si or GaAs wafer suitable for use in semiconductor fabrication processes known in the art.

[0029] The quantum dots can be formed from various materials and have a wide range of dimensions provided the QDs have energy levels to absorb IR energy in the solar spectrum. In an embodiment, the QDs absorb at least a portion of energy having a wavelength of 700 nm to 1 mm, including all ranges therebetween. Examples of suitable materials include, but are not limited to, InAs, GaAs, Ge, SiGe, CdS, InP, PbSe, GaN, or a

combination thereof. The height, width, and areal density of the quantum dots depends on the materials and growth conditions used to form the quantum dots and are not limited to any specific range. Generally, quantum dots having a height (measured normal to the surface on which the quantum dots are disposed) of from 2 nm to 10 nm, including all values to the nm and ranges therebetween. For example, a height of from 3 nm to 5 nm is desirable for InAs quantum dots. The length and width of the quantum dots can be from 10 nm to 40 nm, including all values to the nm and ranges therebetween. A broad range of quantum dot densities can be used. For example, the density of quantum dots can be from  $10^{10}$  to  $10^{12}$  cm<sup>-2</sup>, including all values to the cm<sup>-2</sup> and ranges therebetween. The quantum dots can be formed by methods known in the art. For example, the quantum dots can be formed by self-assembly methods. Examples of self-assembly methods include the Stranski-Krastanow and Volmer-Weber methods.

5

10

15

20

25

30

[0030] A wide quantum dot size (e.g., length, width, and height) distribution can be used. For example, the relative full-width at half maximum (FWHM) of the quantum dot size (e.g., length, width, or height) distribution can be from 10% to 70%, including all integer % values and ranges therebetween.

[0031] The layers of semiconductor materials (e.g., the first, second, or third semiconductor layers) can be formed from a variety of semiconductor materials. Such materials are semiconducting. Examples of suitable semiconductor materials include, but are not limited to, GaAs, InP, Si, BaF<sub>2</sub>, CaF<sub>2</sub>, and SiC. The semiconductor layers can have a broad range of thicknesses. For example, the layers can, each independently, be from 0.2 micrometers to 10 micrometers, including all values to the 0.1 micrometer and ranges therebetween. The layers can be n-doped or p-doped as desired. The doping level is within the purview of one having skill in the art.

[0032] The layer of semiconductor material in which the quantum dots are disposed is n-doped. This layer can be referred to as the quantum dot medium. Devices with such n-doping have increased the conversion efficiency as compared to the same device without such n-doping or direct doping of QDs. For example, the quantum dots disposed in the quantum dot medium can be a planar layer of quantum dots in a layer of n-doped semiconductor material. The quantum dots can be randomly placed in the QD layer. In an embodiment, the positions of the quantum dots in the QD layer are not regular.

[0033] The quantum dot medium can be formed by methods known in the art. For example, the n-doped layer of semiconductor material can be produced during the formation of the semiconductor material layer using molecular beam epitaxy (MBE) or metal-organic

chemical vapor deposition (MOCVD) methods. It is considered that having multiple QD medium layers where the distance between the QD layers is greater than 30 nm will not result in intermediate band formation. In an embodiment, the device does not have intermediate bands.

5 [0034] Without intending to be bound by any particular theory, it is considered that conversion efficiency improves if the doping level corresponds to two or more electrons per dot. By "electrons per dot" it is meant that the amount of dopant averaged over the QD medium corresponds to the number of electrons per dot. For example, the doping level can correspond to two electrons per dot to thirty electrons per dot, including all integer electrons per dot values and ranges therebetween. Thus, in various embodiments, the layer is n-doped such that the dopant concentration in the layer is equivalent to at least two electrons per dot, at least three electrons per dot, at least four electrons per dot, at least five electrons per dot, or at least six electrons per dot. In an embodiment, the device has a doping level corresponding to six electrons per dot and exhibits a 50% increase in efficiency compared to devices that have layers which are not n-doped.

[0035] In an embodiment, the n-dopant in the quantum dot medium is substantially localized in a discrete region of the QD medium semiconductor material. This discrete region can have a thickness of from 1nm to 100 nm, including all values to the nm and ranges therebetween. For example, this discrete region can be a selectively-doped layer or a  $\delta$ -doped layer within the QD medium layer. Without intending to be bound by any particular theory, it is considered that devices with such regions or layers have increased potential barriers around the dots. Such devices have increased conversion efficiency as compared to the same device without such n-doping.

20

30

[0036] In an embodiment, the layer of quantum dot medium comprises a discrete sub-layer of a plurality of quantum dots and a discrete sub-layer (e.g., a selectively-doped layer or a δ-doped layer) of n-doped second semiconductor material in the second semiconductor material. In an embodiment, the n-dopant in the QD medium layer is only in a discrete region or discrete sub-layer (e.g., a selectively-doped layer or a δ-doped layer) of the semiconductor material.

[0037] By "substantially localized" it is meant at least 90% of the n-dopant in the QD medium layer is in a discrete region or a discrete sub-layer of the semiconductor material. In various embodiments at least 95%, at least 96%, at least 97%, at least 98%, at least 99% or 100% of the n-dopant is in the region or layer of the semiconductor material.

[0038] The  $\delta$ -doped layer is a discrete sub-layer of n-doped semiconductor material in the QD medium semiconductor material. This layer can have a thickness of from 1 nm to 10 nm, including all values to the nm and ranges therebetween. For example, the  $\delta$ -doped layer boundary can be from greater than or equal to 5% of the total thickness of the QD medium layer from either boundary of the QD medium layer. For clarity, if the thickness of the layer is 100 nm, the  $\delta$ -doped layer boundary can be from 5 nm or greater from either boundary of the QD medium layer. In another example, the center of the  $\delta$ -doped layer is substantially equidistant from either boundary of the QD medium layer. In this instance, by "substantially equidistant" it is meant that the center of the  $\delta$ -doped layer is at a distance of 10% or less of the total thickness of the QD medium layer from the center of the QD medium layer. In various embodiments, the center of the region is at a distance of 5% or 1% or less from the center of the layer.

5

10

15

20

25

30

[0039] In an embodiment, the stack of layers comprises a plurality of quantum dot medium layers. For example, the stack can have from 2 to 100 individual layers of semiconductor material having quantum dots disposed in the material, including all integer number of layers and ranges therebetween. There is no requirement that intermediate bands be formed. Thus, in an embodiment, the thickness of the layers is such that intermediate bands are not formed. In an embodiment, the thickness of the inter-dot space layers is large enough (e.g., 20 nm or greater in InAs QD/GaAs structures) to minimize stress and formation of defects, which increase recombination losses.

[0040] Optionally, the device can comprise other layers. For example, the device can comprise layers such as electrodes, anti-reflecting coating layer, and back-surface field barriers. The device can be used in combination with solar energy concentrators.

[0041] The devices can demonstrate improved harvesting of IR energy. For example, when compared to devices without quantum dots with built-in charge, the devices of the instant invention show an improvement of 50% of efficiency due to conversion of IR energy. In various embodiments, the device is a photovoltaic device exhibiting an improved conversion efficiency of at least 5%, 10%, 20%, 30%, 40% or 50%, as compared to a photovoltaic device that does not have quantum dots with built-in charge.

[0042] The devices can also demonstrate improved short circuit,  $J_{SC}$ , values. For example, the short circuit current density of the device increases to 24.3 mA/cm<sup>2</sup> without deterioration of the open circuit voltage, compared to 15.1 mA/cm<sup>2</sup> in an undoped solar cell. In various embodiments, the short circuit,  $J_{SC}$ , values for Q-BIC GaAs devices are from 15 mA/cm<sup>2</sup> to 35 mA/cm<sup>2</sup>, including all values to the mA/cm<sup>2</sup> and ranges therebetween.

[0043] In another aspect, the present invention provides methods of making devices (e.g., photovoltaic devices) that have quantum dots with built-in charge. In an embodiment, a method for making a device comprises the following steps of: a. providing a semiconductor substrate; b. depositing a layer of n-doped first semiconductor material or p-doped first semiconductor material on the substrate; c. fabricating a layer of quantum dot medium; and d. depositing a layer of p-doped semiconductor material, if n-doped material is deposited in step b., or depositing a layer of n-doped material, in p-doped material is deposited in step b. In an embodiment, the present invention provides a device made by a method of the present invention.

5

20

25

30

10 [0044] The layer of quantum dot medium is fabricated by: a. depositing a first layer of second semiconductor material; b. depositing a layer of quantum dot material, such that a plurality of quantum dots is formed; and c. depositing a second layer of second semiconductor material and n-doping the layer, or depositing a second layer of second semiconductor material such that the second layer of second semiconductor material is n-doped. Optionally, steps a., b., and c. are repeated. For example, the steps can be repeated from 2 to 100 times.

[0045] The semiconductor materials can be deposited by methods known in the art. For example, the layers of semiconductor material can be deposited by MBE or MOCVD methods. The layers can be doped (e.g., n-doped or p-doped) by methods known in the art. The layers can be doped during deposition or after deposition. Determining conditions which result in the desired doping levels for the various layers is within the purview of one having skill in the art.

[0046] The quantum dot material is the material from which the quantum dots are formed. For example, a layer of InAs is deposited to form InAs quantum dots. The quantum dot material can be deposited by methods known in the art.

[0047] In an embodiment, the layer of second semiconductor material is selectively doped. For example, a n-doped layer of second semiconductor material can be formed by depositing a discrete region (e.g., a selectively-doped layer or a  $\delta$ -doped layer) of n-doped second semiconductor material as part of the deposition of the layer of second semiconductor material. In an embodiment, the layer of quantum dot medium (e.g., having a selectively-doped layer or a  $\delta$ -doped layer) is fabricated by: a. depositing a first layer of second semiconductor material; b. depositing a layer of quantum dot material, such that a plurality of quantum dots is formed; c. depositing a second layer of second semiconductor material; d. depositing a third layer of second semiconductor material, such that the layer is n-doped; and

e. depositing a fourth layer of second semiconductor material. Optionally, steps a., b., c., and d. are repeated. For example, the steps can be repeated from 2 to 100 times.

[0048] The quantum dots can be formed by a variety of methods known in the art. The quantum dots can be formed using methods based on self-assembly, such as, for example, the Stranski-Krastanow or Volmer-Weber methods. The Stranski-Krastanow method is an epitaxial method that efficiently creates a lattice-mismatch strain between the dots and the bulk matrix while minimizing lattice damage and defects. This method is sometimes referred to as the "self-assembled quantum dot" technique. In this method, the self-assembled quantum dots appear spontaneously, substantially without defects, during crystal growth with MOCVD or MBE. Using growth conditions of the Stranski-Krastanow method, it is possible to create arrays of quantum dots with high sheet density (>10<sup>10</sup>cm -2).

[0049] In an embodiment, the quantum dots are deposited by a self-assembly method. For example, 1.7 to 3.5 monolayers of a material such as InAs are deposited on a layer of semiconductor material such that quantum dots grow spontaneously.

[0050] Optionally, the method can comprise additional steps. For example, the method can comprise deposition of layers such as electrodes, anti-reflecting coating layer, and back-surface field barriers.

[0051] The following example is presented to illustrate the present invention. It is not intended to limiting in any manner.

20 EXAMPLE

5

10

15

25

30

[0052] A 50% increase in the power conversion efficiency of InAs/GaAs quantum dot solar cells due to n-doping of the inter-dot space was demonstrated. The n-doped device was compared with GaAs reference cell, undoped, and p-doped devices. It was found that the quantum dots with built-in charge (Q-BIC) enhance electron intersubband quantum dot transitions, suppress fast electron capture processes, and preclude deterioration of the open circuit voltage in the n-doped structures. These factors lead to enhanced harvesting and efficient conversion of IR energy in the Q-BIC solar cells.

[0053] The effects of the quantum dot recombination processes were investigated. Two straightforward ideas that support this research are related to the expected positive effects of doping on  $V_{OC}$  and IR harvesting. First, it was anticipated that, as in conventional heterojunction devices, doping will avert the deterioration of the open circuit voltage. Second, it was also expected that additional carriers in QDs created by doping would enhance the IR absorption and the photocurrent as shown in Figure 3 for n-doping. Figure 3a presents

the processes in a QD structure without doping. Figures 3b and c show the doping-induced process associated with electrons in the ground state due to intentional doping of dots. Figure 3c demonstrates a two-step process, where two electrons are excited by IR radiation to the excited localized QD state. Consequently, strong electron-electron interaction in QDs causes one of these electrons to transfer to some low-energy state (for example, to the ground state) while another electron transfers to the conducting state and leaves the dot. The n-doping enhances electron transitions in QDs shown in Figures 3b and c without substantially changing the hole kinetics. In the same way, the p-doping enhances the hole transitions in QDs. Comparing electron and hole transitions in QDs, one should take into account that the electron energy level spacing in QDs is significantly larger than the spacing for holes due to the large effective mass of holes. The electron transitions in QDs significantly exceed the thermal energy and cannot be induced by thermal phonons. To stimulate these transitions by IR radiation, the n-doping should be preferable.

5

10

15

20

25

30

[0054] A critical and challenging question that needs to be addressed is the effect of doping on the photocarrier capture rate and dot population. Like the quantum well population, the dot population under a stationary light flux is determined by the condition of equal capturing for electrons and holes into a dot. Different electron and hole capture rates lead to an accumulation of the built-in charge and creation of potential barriers, which impede fast capture processes and accelerate slow processes. Thus, the dot population under light is determined by both doping and the carrier capture rates. There is a strong dependence of capture rates on the electric field even in relatively small fields. Consequently, the built-in charge substantially affects the effective electric field around the dot thereby modifying capture processes. Thus, the harvesting of IR radiation (Figures 3b,c) and carrier capture are strongly interrelated via the built-in charge and corresponding barriers around dots.

[0055] To study effects of the built-in charge on the  $J_{SC}$ ,  $V_{OC}$ , and efficiency, as well as to understand the IR-induced transitions and capture processes, p-and n-doped InAs/GaAs QD solar cells with various doping levels were fabricated and investigated. The *I-V* characteristics under light, spectral response, and photoluminescence were measured. Finally, the data that shows the dependencies of solar cell parameters on doping was collected. The results show that n-doping of the inter-dot space improves solar energy conversion. For the most heavily doped sample, the photovoltaic efficiency improves by as much as 50% compared with an undoped device. Because no evidence of the effect saturating was

observed, it is considered that an even stronger enhancement of the photovoltaic efficiency for further increase of the doping level can be achieved.

[0056] Figure 2 shows the growth diagram of a delta ( $\delta$ )-doped QD structure in which a plane of dopants is placed in the middle of each GaAs layer that separates the dot layers.

5

10

15

20

25

30

The structures were grown on n+-GaAs (100) substrates by molecular beam epitaxy. Following oxide desorption, a 300 nm n+-GaAs buffer with a doping density of  $10^{18}$ cm<sup>-3</sup> was grown at 595°C. The substrate was cooled down to 530 °C for growth of the solar cell structure. QD growth occurred following the deposition of 2.1 monolayers (MLs) of InAs. The structures contain 20 stacks of QD layers separated by GaAs with dopant sheet densities of 0,  $2.4 \times 10^{10}$ ,  $3.6 \times 10^{10}$ ,  $4.8 \times 10^{10}$ , and  $7.2 \times 10^{10}$ cm<sup>-2</sup> for providing zero, two, three, four, and six electrons per QD, respectively (based on average dot densities measured with transmission electron microscopy). The thickness of the GaAs spacer layer was 50 nm for all samples. The spacer thickness was chosen in an effort to dissipate strain fields in subsequent layers and hence reduce the strain accumulation and dislocations in the multistack samples.

These relatively large spacers completely suppress electron tunneling between dots and prevent formation of the intermediate band. It will be shown that the localized levels in QDs provide efficient IR harvesting. The p+- $\delta$ -n+ structure (where  $\delta$  refers to the  $\delta$ -doped quantum dot layers) was completed by a 100 nm p-GaAs with a doping density of  $1 \times 10^{18} \text{cm}^{-3}$ , 30 nm p-Al<sub>0.45</sub>Ga<sub>0.55</sub>As with a doping density of  $5 \times 10^{18} \text{cm}^{-3}$ , and finally a 50 nm p-GaAs contact layer with a doping density of  $5 \times 10^{18} \text{cm}^{-3}$ .

[0057] For characterization of the device performance, 250 μm circular solar cells were fabricated using standard photolithography followed by a phosphoric acid wet chemical etching. The structure was etched down into the n+-GaAs substrate. Subsequently, an n-type blanket metallization of gold/tin/gold (15 nm/25 nm/250 nm thicknesses, respectively) was performed in an electron beam vacuum evaporator onto the back side of the substrate. Following blanket metallization, a rapid thermal annealing at 375 °C for 60 s was performed. Finally, the top of each mesa was patterned with a p-type metal ring contact. A chromium/gold contact layer (25 nm/250 nm thick, respectively) was deposited followed by a metal lift-off. The contact ring diameter is 200 μm with a 100 μm opening in the center to allow for top-side illumination. An array of these mesas was cleaved from the wafer and mounted in a 68 pin leaded chip carrier (LDCC) using indium metal. Wire bonds were attached to the top contact metal and out to a pin connection on the LDCC.

[0058] The *I-V* characteristics of the devices were measured under light using a Newport Oriel PV calibrated solar simulator, which provides 1 Sun (AM1.5G) illumination. An Agilent 4156C precision semiconductor parameter analyzer was used to obtain the *I-V* curves that are shown in Figure 5. Solar cell parameters such as the J<sub>SC</sub>, V<sub>OC</sub>, the fill factor FF, and the cell efficiency have been obtained from the resulting curves. While the p-doped device with the doping density of 4.8 × 10<sup>10</sup> cm<sup>-2</sup> shows degradation in J<sub>SC</sub> compared with the undoped device, the n-doped devices show a monotonic increase in J<sub>SC</sub> with increasing of the doping level. Table 1 shows that, compared with the undoped device, the power conversion efficiency increases by 4.5, 30, and 50% for doping levels of 2, 3, and 6 electrons per dot, respectively.

Table 1. QD Solar Cell Parameters

15

The built-in- dot charge	Short circuit current J <sub>SC</sub> (mA/cm <sup>2</sup> )	Open circuit voltage Voc (V)	Fill factor (%)	Conversion efficiency
				(%)
0	15.1	0.77	77	9.31
2	17.3	0.74	76	9.73
3	18.5	0.79	75	12.1
6	24.3	0.78	72	14.0

[0059] In order to determine the harvesting role of IR photons in this radical improvement of the photovoltaic conversion efficiency, the spectral dependence of the photocurrent was measured under low illumination conditions using a Nicolet Fourier transform infrared (FTIR) spectrometer. Figure 6 shows the photoresponse of the GaAs reference cell, the undoped QD solar cell, and the QD solar cells doped to provide 2 electrons per dot. The band-to-band absorption in the GaAs matrix (E<sub>m</sub> in Figure 3a) is observed below 880 nm. Transitions in the range from 880 to 920 nm correspond to the wetting layer.

Transitions above 920 nm are most likely related to the various excited QD states (e.g., E<sub>1</sub> in Figure 3a). Finally, the ground state transition in QDs is 1100 nm (E<sub>0</sub> in Figure 3a). As seen, the photoresponse due to short-wavelength (above bandgap of GaAs) photons is reduced due to QDs, while the photoresponse contribution due to long-wavelength photons is enhanced. Doping further reduces the short-wavelength photoresponse related to the band-to-band

transitions and transitions in the wetting layer but substantially enhances the IR photoresponse via QDs. The spectral density of the photocurrent monotonically decreases when the radiation wavelength increases up to 4.8  $\mu m$ . As seen from the inset to Figure 6b for the sample with six electrons per dot, the spectral density shows a sharp rise at 4.8  $\mu m$  (250 meV), which is believed to correspond to the transition from the dot ground state to the low energy resonance conducting state ( $E_{isb}$  in Figure 3b). In addition, a broad weak peak is observed between 4.8 and 8  $\mu m$ , which is close to the cutoff of the experiment. This peak decreases with doping decrease and is completely absent in the reference cell. Note that the analogous spectral dependencies and dependencies on doping have been observed in absorption of QD structures.

5

10

15

20

25

30

goetrum to the photoresponse of the present devices, the photocurrent under 1 Sun radiation was measured using a GaAs filter, which eliminates photons with wavelengths less than 880 nm. The *I-V* characteristics obtained with this filter, which were corrected for reflectivity losses, are presented in Figure 7. As expected, the GaAs reference cell does not show any photoresponse to the long-wavelength part of solar spectrum. The photoresponse due to radiation at wavelengths greater than 880 nm significantly increases with doping. In the device doped to provide two electrons per dot, an increase in the photocurrent of 7.0 mA/cm<sup>2</sup> was observed compared with the reference cell. The photocurrent from the sample with 6 electrons per dot increased by 9 mA/cm<sup>2</sup>.

[0061] To study the effect of high energy photons on IR harvesting, the IR photoresponse of QD structures under short-wavelength radiation was also investigated. The InAs/AlGaAs QD structures were doped with Si in the middle of AlGaAs layers with a doping sheet concentration of  $2.7 \times 10^{11}$  cm<sup>-2</sup>. A red LED with 620 nm wavelength was used for optical pumping. Figure 8 shows the photocurrent induced by 4300 nm IR radiation that corresponds to intersubband transitions in QDs. The measurements at 78 K demonstrate the increase of photocurrent by orders of magnitude due to the short-wavelength pumping. This observation manifests the strong enhancement of the IR electron transitions from the localized states in QDs to the conducting states in the matrix. Let us note that the QD structures used in these measurements were designed for IR photodetectors with large (up to 100) photoconductive gain, g, which strongly increases the photoresponse.

[0062] To investigate mechanisms of carrier capture and evaluate effects of doping on the recombination losses, the room temperature photoluminescence (PL) was studied in the

solar cells under short circuit conditions to match the conditions of previous *I-V* measurements. The 532 nm line from a frequency-doubled neodymium doped yttrium aluminum garnet (Nd:YAG) laser was used to stimulate PL transitions. The diameter of the laser spot on a sample was 20 µm. The PL signal from the sample was dispersed by a monochromator and detected by an InGaAs detector array. The PL spectra were taken at 0.3 W/cm² excitation intensities. Figure 9a shows the dependence of the PL on the doping level in n-doped samples. The PL intensity substantially increases with doping. This observation is associated with enhancing of intra-dot relaxation processes via electron-electron and hole-electron scattering in QDs due to electrons trapped in the dots.

5

10

15

20

25

30

[0063] Figure 9b shows the PL of p-and n-doped samples with the same level of doping, which corresponds to four carriers per dot. As seen, the PL intensity from the p-doped sample exceeds that of the n-doped sample by approximately 8 times. Thus, the p-doping substantially enhances capture and relaxation processes and increases the recombination losses. This observation is in agreement with experimental works in the area of QD lasers and light-emitting diodes, where it is well established that the p-doping strongly decreases the photocarrier lifetime and improves the efficiency of light-emitting diodes and modulation speed of QD lasers. Contrary to these devices, the QD solar cells require a long photocarrier lifetime. Therefore, n-doping proves to be more desirable for QD solar cells. In addition, the PL maximum of the p-doped sample is shifted toward the shorter wavelength regime with respect to the corresponding maximum for the n-doped sample. The observed energy shift of approximately 10 meV indicates substantial accumulation of holes in the p-doped QD structures.

[0064] The most pronounced result of employing Q-BIC structures is the radical improvement of the photovoltaic efficiency due to enhanced harvesting of the IR portion of solar spectrum in n-doped solar cells. As shown in Figure 5, the photocurrent,  $J_{SC}$ , increases from 15.07 to 24.30 mA/cm<sup>2</sup> with increasing dot population. It was also found that  $J_{SC}$  in the undoped QD solar cell is almost the same as that in the GaAs reference cell. The  $J_{SC}$  monotonically increases with increasing n-doping, but decreases due to p-doping. The scope of the data shows that the improvement of QD solar cell due to built-in charge should be associated with the doping-induced electron intersubband transitions, as presented in Figures 3b and c. To effectively contribute to the photovoltaic conversion, an electron and a hole should simultaneously escape from the dot. The energy level spacing for electrons in QDs is relatively large. It substantially exceeds the spacing for holes and the thermal energy. For this

reason, it is precisely the electron intra-dot processes that limit the electron-hole escape from QDs. Thus, it is critically important to enhance the photoexcitation of electrons rather than holes.

5

10

15

20

25

30

[0065] Spectral response measurements in Figure 6 show partial contributions of the band-to-band, wetting layer, QD ground state, and QD subband transitions to the photocurrent. In agreement with the above interpretation, n-doping reduces the photocurrent generated by the band-to-band transitions and transitions in the wetting layer but substantially increases the IR harvesting via electron transitions shown in Figure 3b,c. The measurements of the photoresponse to IR portion of solar radiation (Figure 7) and its comparison with the photoresponse to the entire solar spectrum (Figure 5) demonstrate that even under a lowpower radiation the short-and long-wavelength contributions are not independent and the total photocurrent is significantly larger than the sum of two separate contributions. Let us note that this effect is known for IR QD photodetectors, where the IR response is significantly enhanced by the optical pumping. In previous investigations, optical pumping was limited by relatively low energy quanta, which could generate only electron-hole pairs localized in the QDs. It was concluded that in this case the optical pumping is equivalent to the doping of QDs. The optical pumping with the energy quanta much larger than the GaAs bandgap also enhances by orders of magnitude the IR photoresponse (see Figure 8). The high-energy radiation increases the number of carriers captured into QDs, which in turn significantly enhances the IR electron transitions from localized states in QDs to the conducting states in matrix as it is shown in Figures 3b and c. As discussed above, the same effect provides a significant increase in the photocurrent of Q-BIC solar cells.

[0066] Besides the effect of doping on the generation of mobile electron-hole pairs, doping affects the carrier capture and relaxation processes via the quantum dots with built-in charge. The photocarrier capture into QDs is usually associated with the inelastic processes accompanied by the emission of optical phonons. Despite many potential applications of QD structures in optoelectronics, there is still very limited and controversial information about capture rates for electrons and holes. While in bulk materials the hole relaxation via emission of an optical phonon is faster than the corresponding electron relaxation, the relation between the capture rates in QDs appear to be the exact opposite. Experimental works, where both capture processes have been studied, show in favor of fast electron capture rate.

[0067] As discussed for quantum-well structures by Ridley, a difference in electron and hole capture rates should lead to an accumulation of a charge in the wells and to a

formation of potential barriers around wells. The same effect is expected to be even more pronounced in QD structures.

5

10

15

20

25

30

[0068] To study potential barriers around QDs as a function of dot population, a simulation tool based on the nextnano<sup>3</sup> software, which solves self-consistently Schrodinger and Poisson equations, was used. Figure 10a shows the potential profile in QD structures. As seen, the potential barriers in the QD planes are smaller than those between QD planes. Therefore, the photoelectron capture via thermoexcitation is mainly expected to come from the QD planes. Figure 10b shows the potential barriers around single dots in QD planes as a function of the quantum dot population. According to these results, the barrier height is proportional to the number of electrons trapped in a dot, that is,  $V_b = k_e n$ , where n is the dot population and  $k_e = 2.5$  meV. The coefficient  $k_e$  depends on the dot form and increases for smaller dots. The built-in negative charge suppresses the fast electron capture processes and accelerates the capture of holes. Taking into account an exponential dependence of the capture rates on the built-in charge, the corresponding dot population may be evaluated as  $n_d$ =  $(k_B T)/(2k_e) \ln (\tau_C^P / \tau_C^n)$ . Therefore, even a relatively small difference in initial capture rates may provide a significant built-in charge. For example, for  $\tau_C^P / \tau_C^n = 4$  results in seven electrons localized in the dot. If the built-in charge is not provided by doping, the corresponding charge comes from p+- and n+-contacts and changes the potential profile in the active area. To avoid this negative effect, one should choose the doping level that provides the dot population  $n_d$ , which equates the electron and hole capture rates. These investigations show that effects of doping on processes in Q-BIC solar cells are complex and interrelated. The undoped device demonstrates small, 0.5 mA/cm<sup>2</sup> increase in J<sub>SC</sub> with respect to the GaAs reference cell (Figure 5), while the IR radiation itself gives an increase in the photocurrent of ~4 mA/cm<sup>2</sup> (Figure 7). These data show that in the undoped structures the significant positive effect of IR harvesting by QDs is eliminated by the recombination processes generated by QDs. Note that such small improvements in J<sub>SC</sub> were observed in a number of previous works. The situation radically changes with doping.

[0069] While the recombination processes are enhanced with doping (Figure 9), the doping-induced IR harvesting prevails over the recombination losses. The net positive effect increases with the doping level. At the doping level of two electrons per dot,  $J_{SC}$  increases by approximately 2.5 mA/cm<sup>2</sup> (Figure 5) and the IR radiation itself gives an increase in the photocurrent of approximately 7 mA/cm<sup>2</sup> (Figure 7). This shows that the recombination

losses related to the conversion of short-wavelength radiation decrease the photocurrent by  $4.5 \text{ mA/cm}^2$ . At the doping level of six electrons per dot,  $J_{SC}$  increases by approximately 9 mA/cm<sup>2</sup> (Figure 5) and the IR radiation itself also gives an increase in the photocurrent of approximately 9 mA/cm<sup>2</sup> (Figure 7). However, this coincidence cannot be interpreted as additivity of partial spectral contributions to the photocurrent. At this doping level, the recombination losses related to the conversion of short-wavelength photons turn out to be compensated by the effect of optical pumping in the IR harvesting. As seen from the above discussion, these two effects are significant and require further investigations, in particular, at higher doping levels and higher intensities of radiation. One of the limitations on the doping level may originate due to the Auger recombination, which at the current doping levels remains substantially weaker than the Shockley-Read-Hall recombination.

5

10

15

20

25

30

It should be highlighted that in the present devices, the strong enhancement of the photocurrent occurs without deterioration of the  $V_{\rm OC}$ . This important improvement is exclusively due to the built-in charge. In previous works on structures without doping, even a small increase in  $J_{\rm SC}$  was usually accompanied by a decrease in  $V_{\rm OC}$ . The positive influence of the doping on  $V_{\rm OC}$  is not a specific feature of solely QD solar cells. It is understood for conventional pn-junction solar cells, that the minimum doping level is determined by the requirements of complete energy conversion. In this case, the difference between the Fermi energies of electrons and holes in the active region under radiation should be smaller than the corresponding difference at the contacts. This in turn requires the concentration of majority carriers in the junction area to be at least as large as the concentration generated by illumination. In practice, this condition leads to a doping level of  $\sim 10^{16}$  cm<sup>-3</sup>, which approximately corresponds to the doping in the present structures.

[0071] It was established that the quantum dots with built-in charge enhanced harvesting of IR energy. As it is summarized in Table 1, in Q-BIC solar cells the efficiency of the photovoltaic conversion increases from 9.3% in devices without doping to 14% in devices with the doping to provide six electrons per dot, which was the maximal doping level in these investigations. It should be noted that the positive effect of Q-BIC is still far from saturation, that is, it is considered that further improvements can be expected with higher doping levels. The improvement of IR harvesting is anticipated to be even stronger at higher radiation intensities due to optical pumping effect. This makes the Q-BIC solar cells promising candidates for use with concentrators of solar radiation.

[0072] While the invention has been particularly shown and described with reference to specific embodiments (some of which are preferred embodiments), it should be understood by those having skill in the art that various changes in form and detail may be made therein without departing from the spirit and scope of the present invention as disclosed herein.

5

#### WHAT IS CLAIMED IS:

1. A device comprising a plurality of quantum dots disposed in a n-doped semiconductor material, such that the quantum dots have built-in charge,

- 5 wherein the charge in the quantum dots creates potential barriers which prevent photoelectron capture by the quantum dots, and wherein the electrons in the charged dots provide coupling to infrared radiation.
- 2. The device of claim 1, wherein the device is characterized by an average built-in-dot charge of at least two electrons per dot.
  - 3. The device of claim 1, wherein the device exhibits a short circuit current of at least 25 mA/cm<sup>2</sup>.
- 15 4. The device of claim 1, wherein the device is characterized by a lack of deterioration of open circuit voltage.
- 5. The device of claim 1, wherein the device does not exhibit intermediate quantum dot bands, and wherein the relative full-width at half maximum of the distribution of QD length or width or height is from 10% to 70%.
  - 6. A device comprising:

25

30

a semiconductor substrate having disposed thereon a stack of layers, wherein the stack of layers comprises,

- a. a layer of n-doped or p-doped first semiconductor material;
- b. a layer of quantum dot medium comprising at least one layer of a second semiconductor material having a plurality of quantum dots disposed therein, wherein the layer of second semiconductor material is n-doped; and
- c. a layer of p-doped or n-doped third semiconductor material, wherein if the first semiconductor material is n-doped the third semiconductor material is pdoped and if the first semiconductor material is p-doped the third semiconductor material is n-doped.

- 7. The device of claim 6, wherein the substrate is GaAs, InP, Si, BaF<sub>2</sub>, CaF<sub>2</sub>, or SiC.
- 8. The device of claim 6, wherein the quantum dots are InAs, GaAs, Ge, SiGe, CdS, InP, PbSe, GaN, or a combination thereof.

5

- 9. The device of claim 6, wherein the n-doped first and third semiconductor material is each individually GaAs, InP, Si, BaF<sub>2</sub>, CaF<sub>2</sub>, or SiC.
- 10. The device of claim 6, wherein the p-doped first and third semiconductor material is each individually GaAs, InP, Si, BaF<sub>2</sub>, CaF<sub>2</sub>, or SiC.
  - 11. The device of claim 6, wherein the layer of second semiconductor material is n-doped at a level of at least two electrons per dot, at least three-electrons per dot, at least four-electrons per dot, at least five-electrons per dot.

15

25

30

- 12. The device of claim 6, wherein the stack of layers comprises a plurality of layers of semiconductor material having a plurality of quantum dots disposed therein.
- 13. The device of claim 12, wherein the stack of layers comprises 10 to 100 layers of semiconductor material having a plurality of quantum dots disposed therein.
  - 14. A method for making a device comprising the steps of:
    - a. providing a semiconductor substrate;
    - b. depositing a layer of n-doped first semiconductor material or p-doped first semiconductor material on the substrate;
    - c. fabricating a quantum dot medium;
    - d. depositing a layer of second semiconductor material, such that the layer of second semiconductor material is n-doped; and
  - e. depositing a layer of p-doped semiconductor material, if n-doped material is deposited in step b., or depositing a layer of n-doped material, if p-doped material is deposited in step b.
  - 15. The method of claim 14, wherein the quantum dot medium is fabricated by:
    - a. depositing a first layer of second semiconductor material;

b. depositing a layer of quantum dot material, such that a plurality of quantum dots is formed;

- c. depositing a second layer of second semiconductor material and n-doping the layer, or depositing a second layer of second semiconductor material such that the second layer of second semiconductor material is n-doped; and
- d. optionally, repeating steps a., b. and c.

5

- 16. The method of claim 15, wherein the steps b. and c. are repeated from 1 to 100 times.
- 10 17. The method of claim 15, wherein the second layer of second semiconductor material is deposited such that the n-dopants are in a discrete region of the second layer of second semiconductor material.
- 18. The method of making a photovoltaic cell of claim 14, wherein step c. is carried out such that the layer of second semiconductor material has at least two electrons per dot, at least three-electrons per dot, at least four-electrons per dot, at least five-electrons per dot, or at least six-electrons per dot.

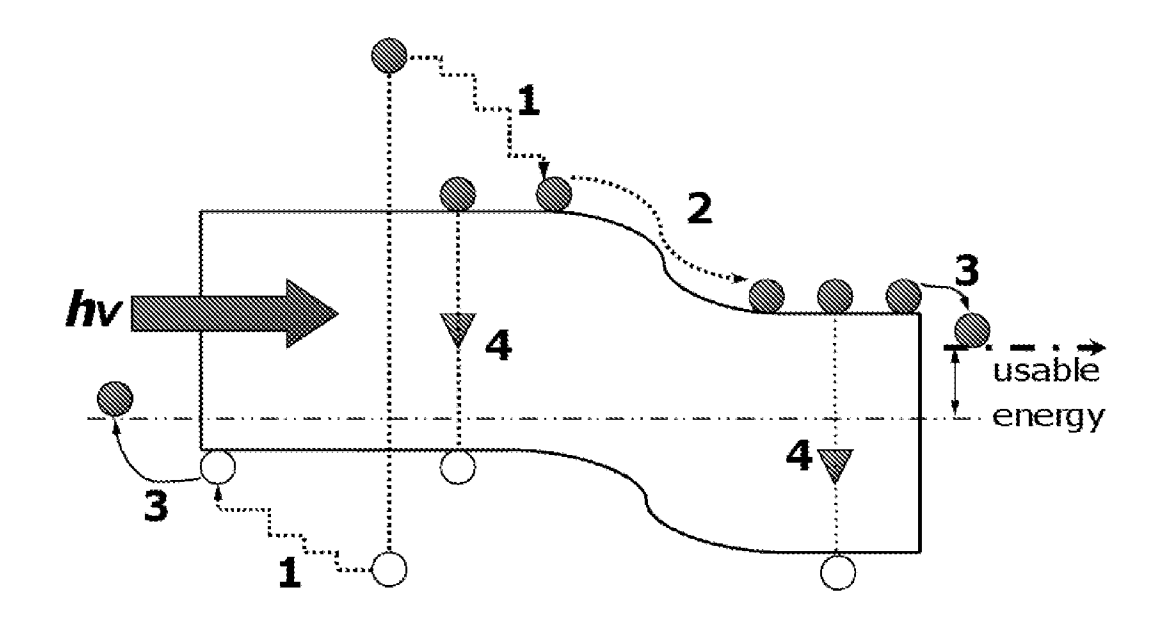


Figure 1

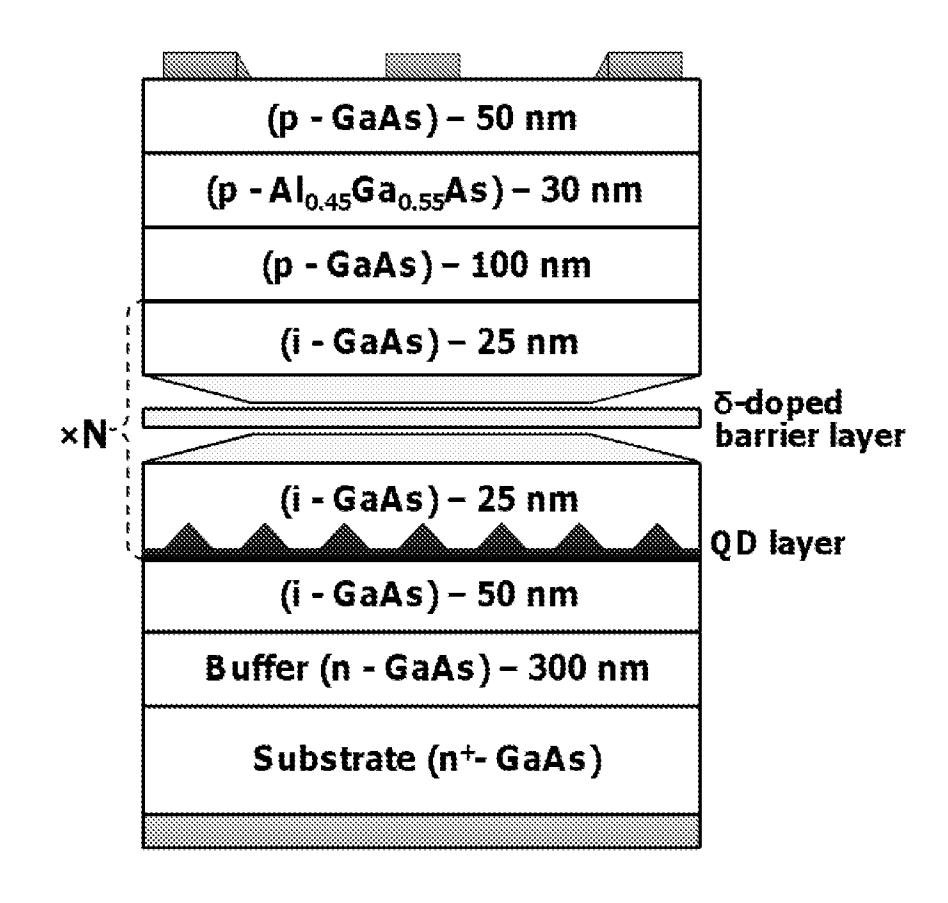


Figure 2

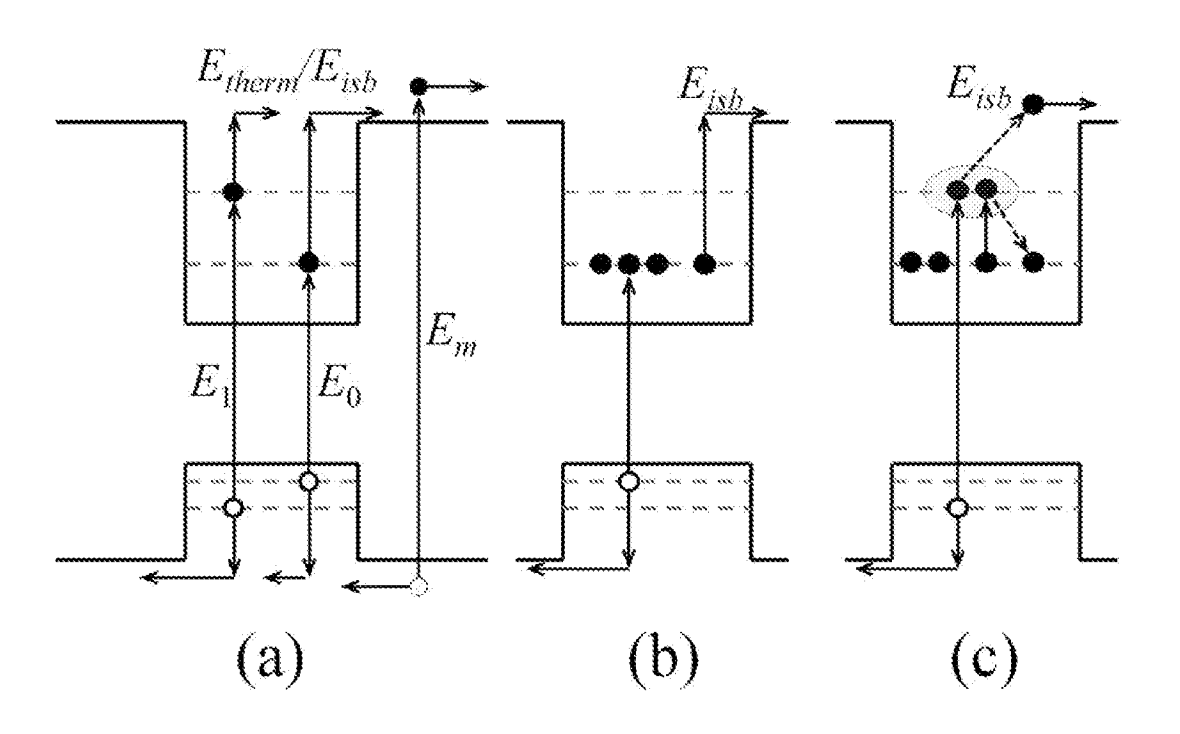


Figure 3

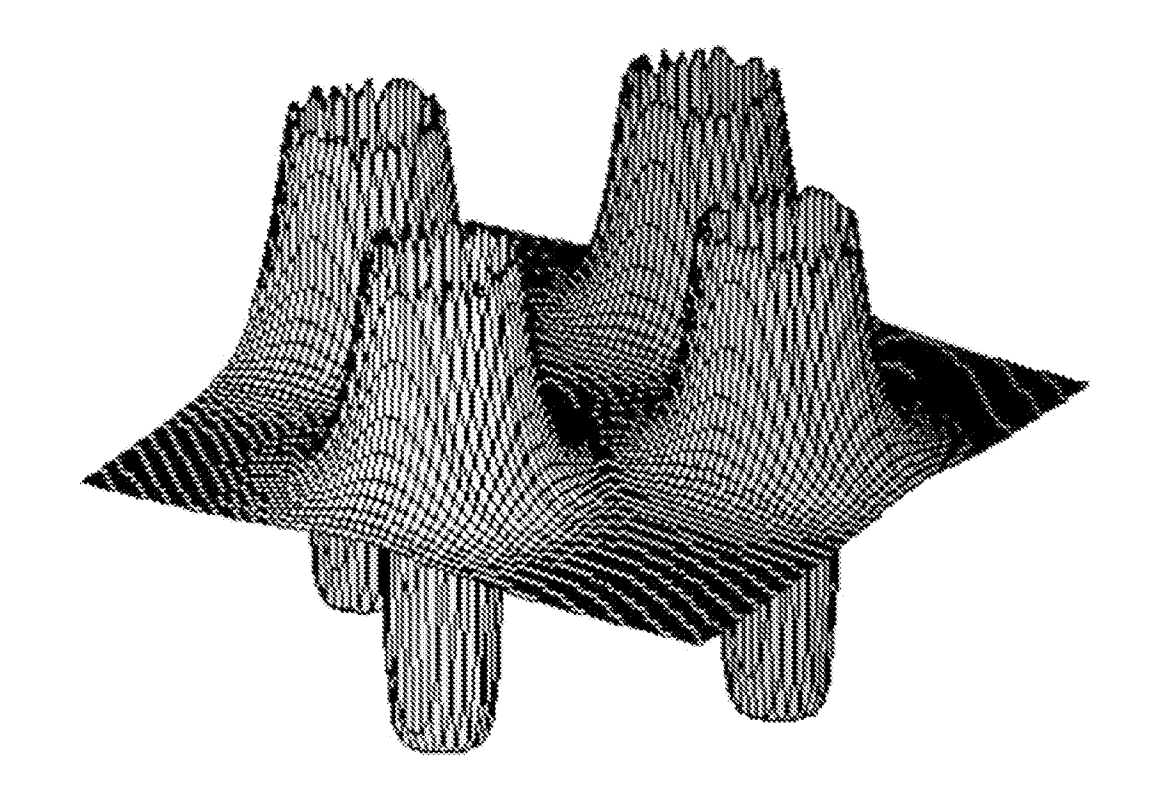


Figure 4

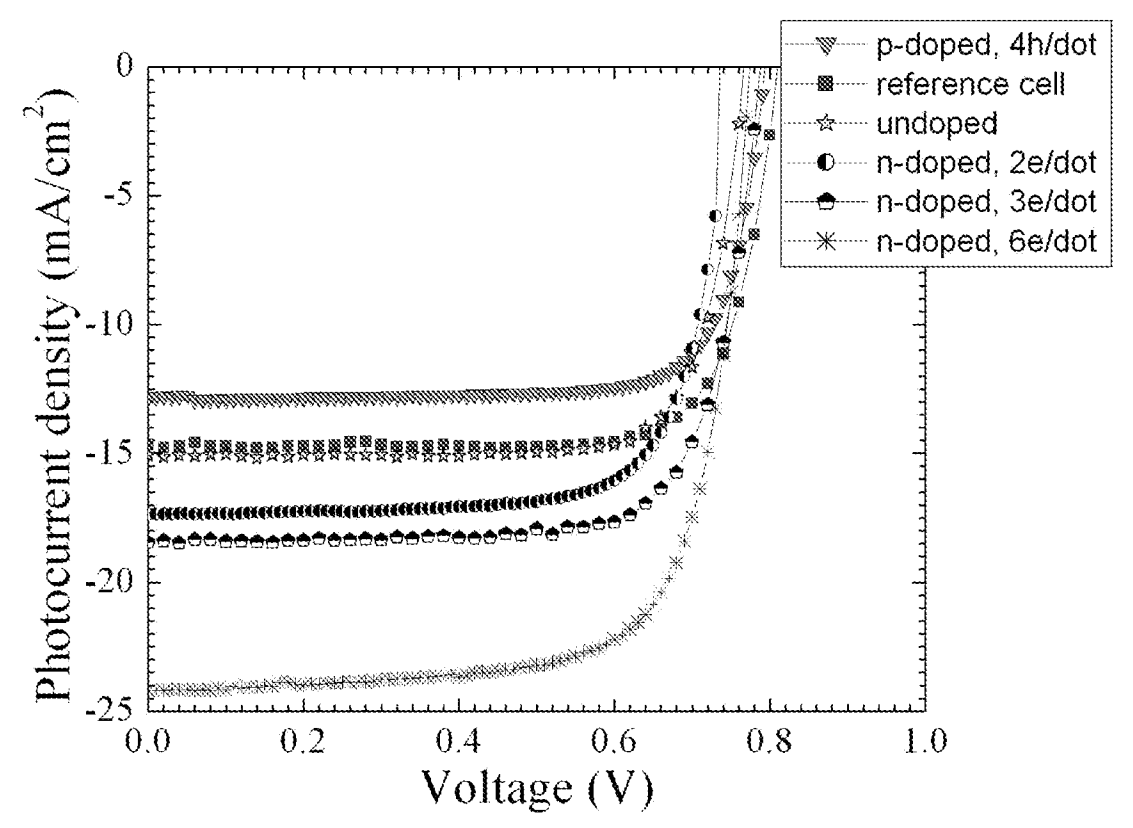
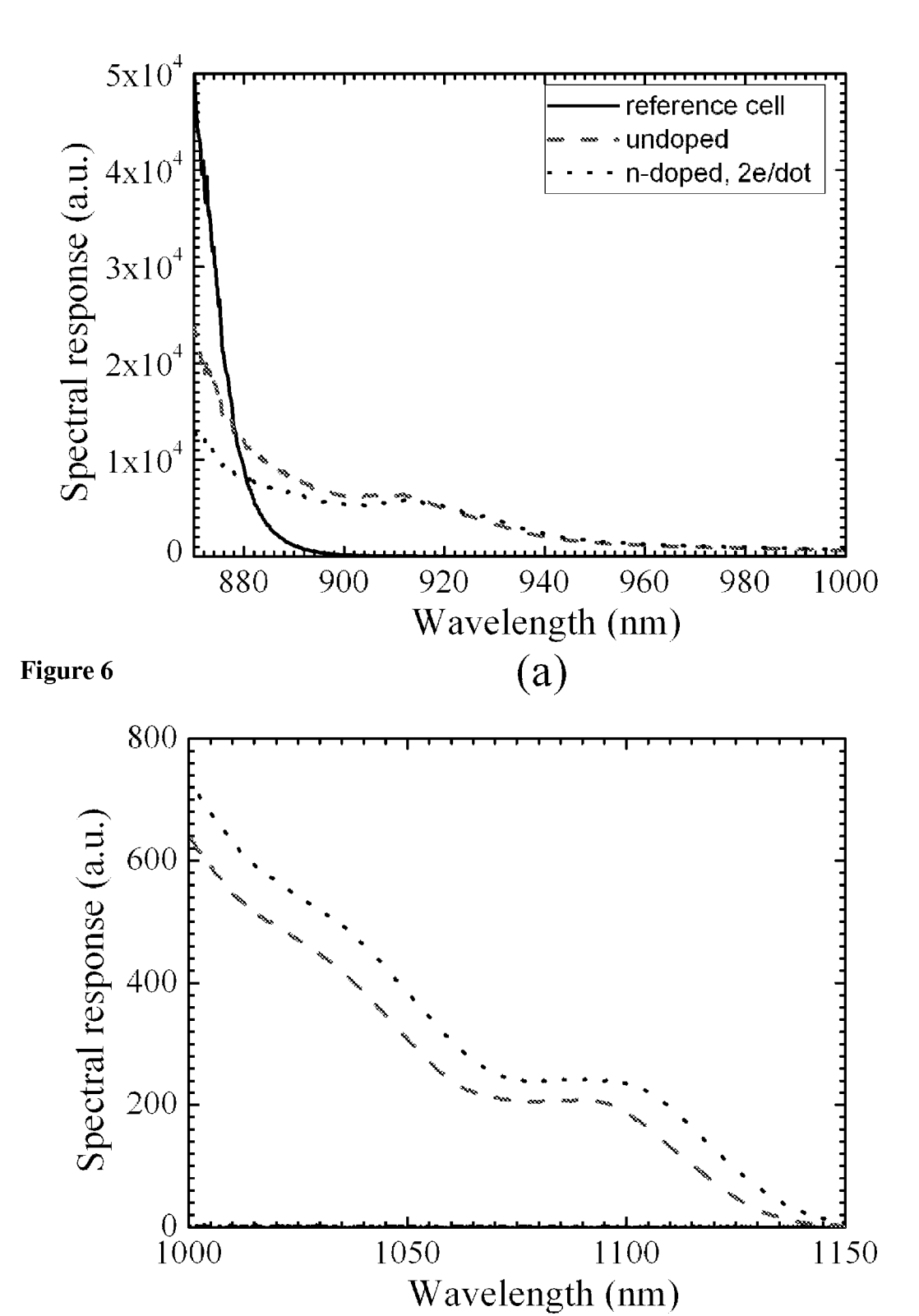


Figure 5

Figure 6



(b)

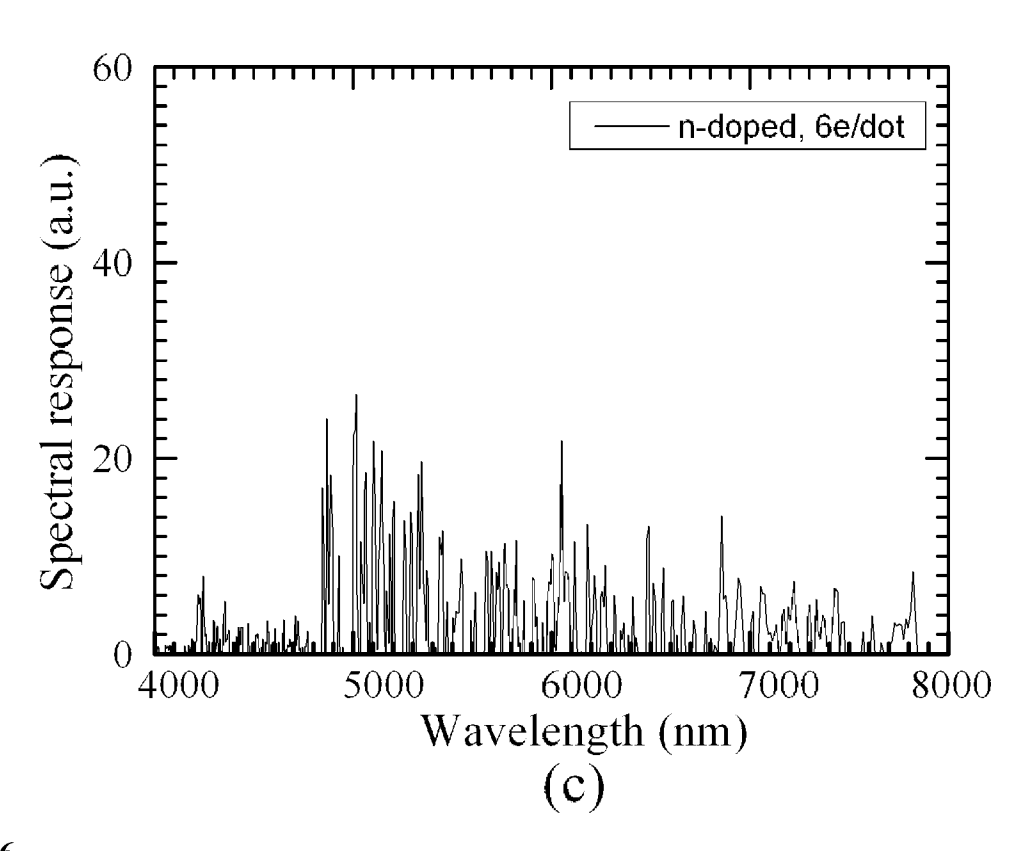


Figure 6

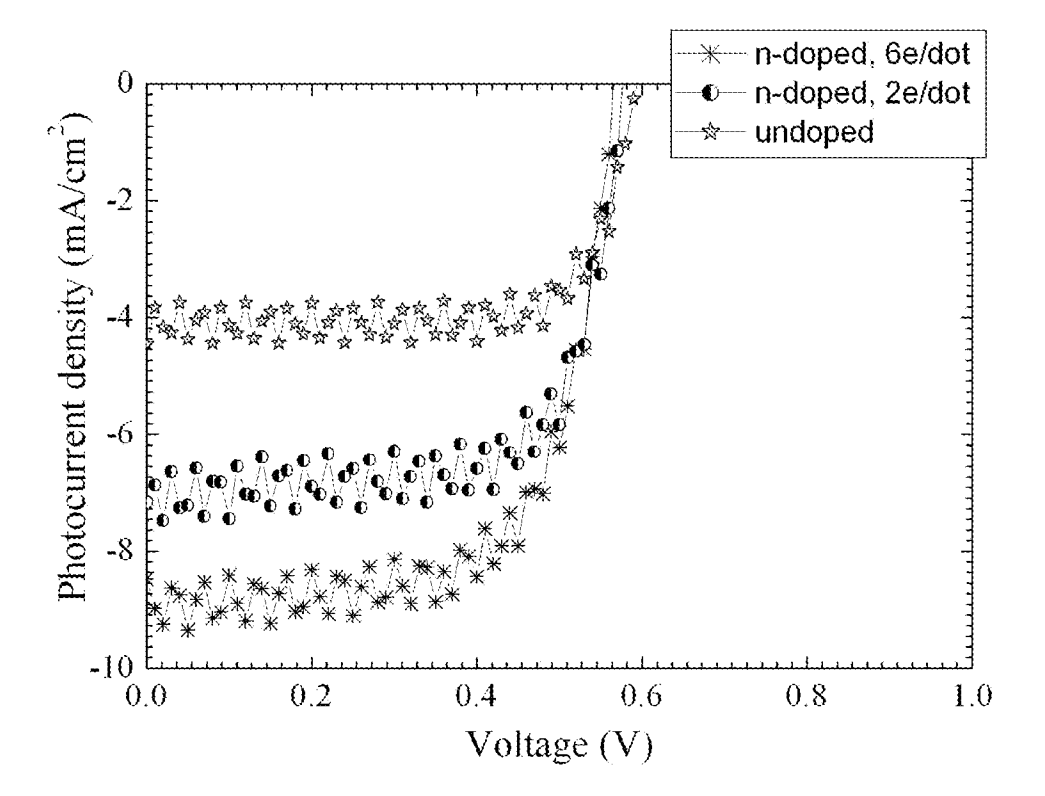


Figure 7

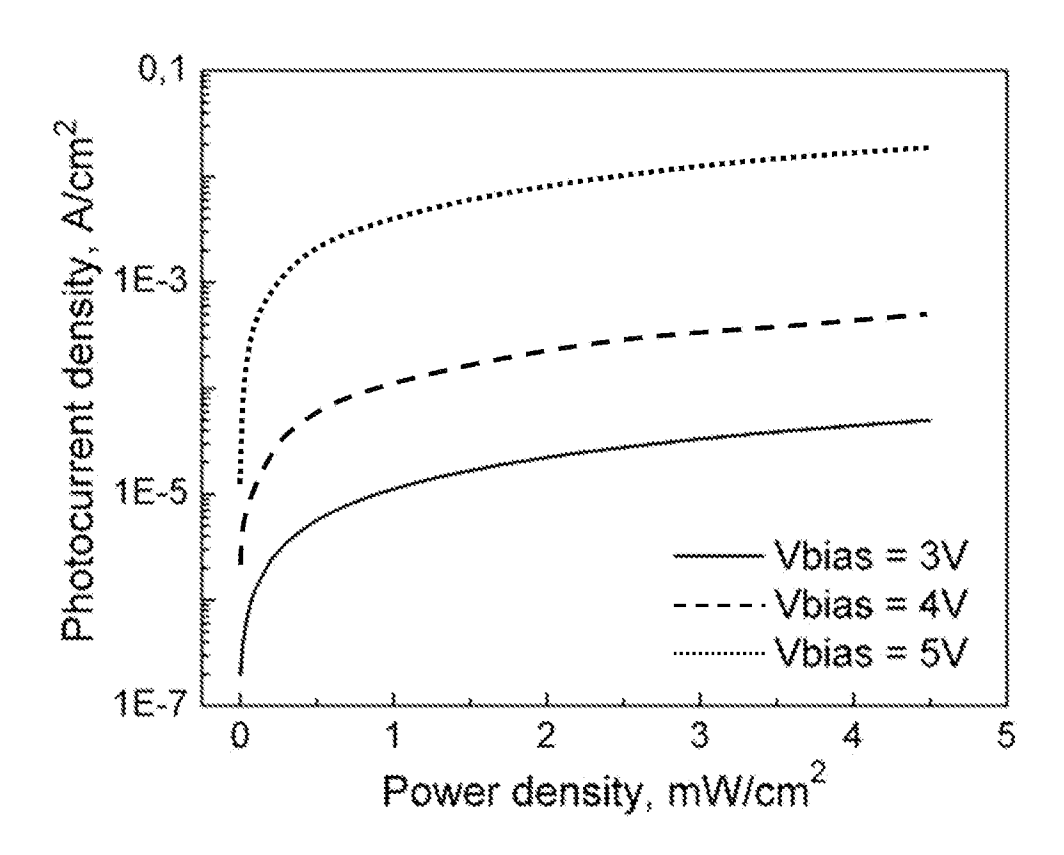


Figure 8

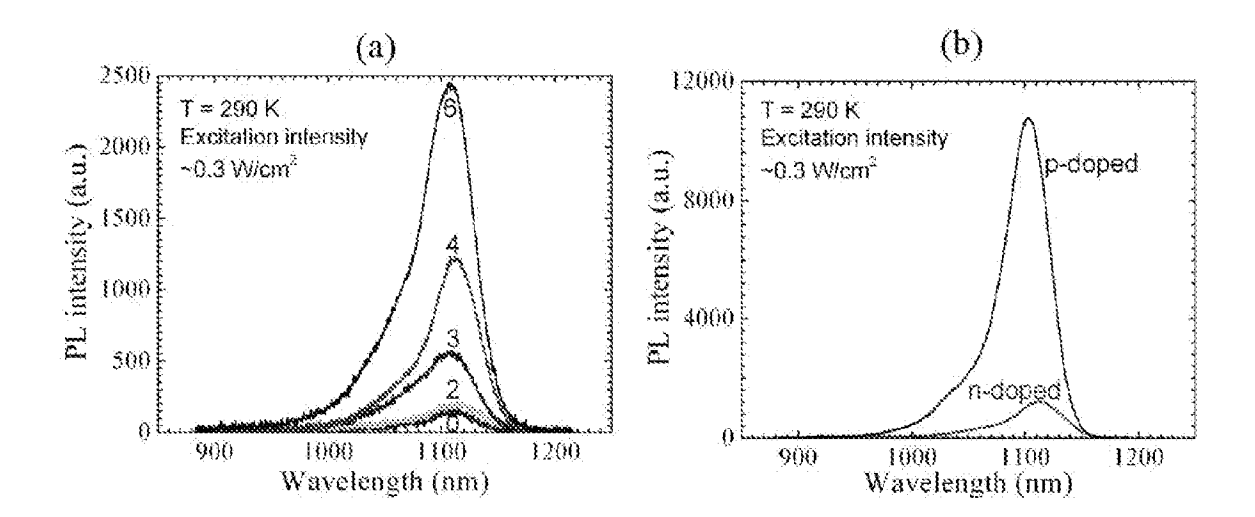
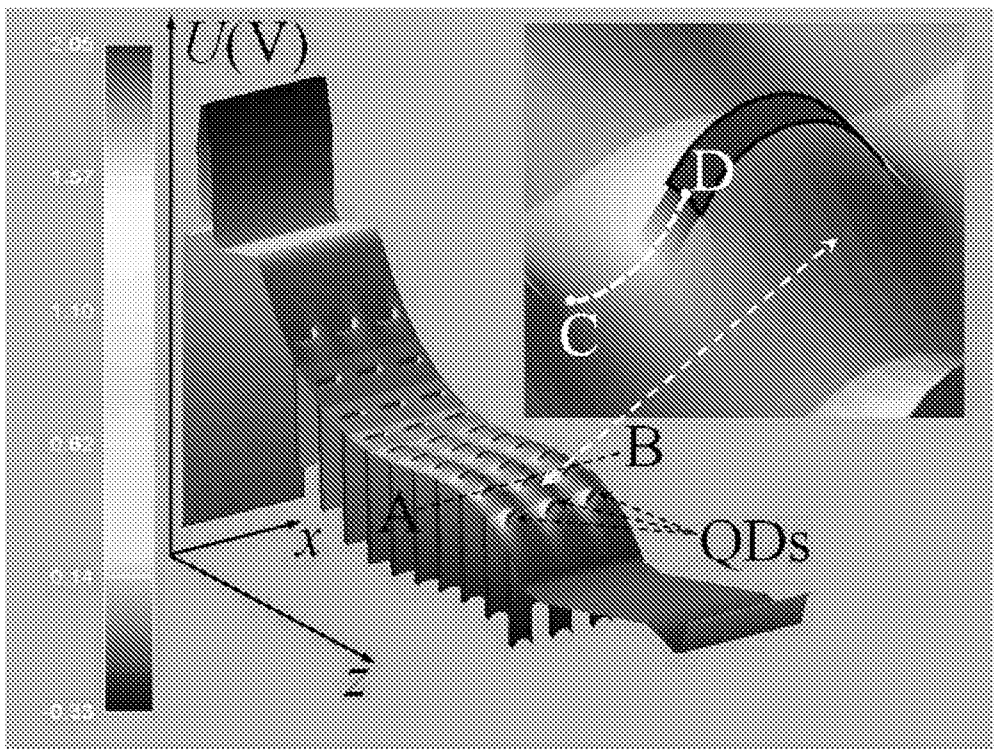


Figure 9

7/7 (a)



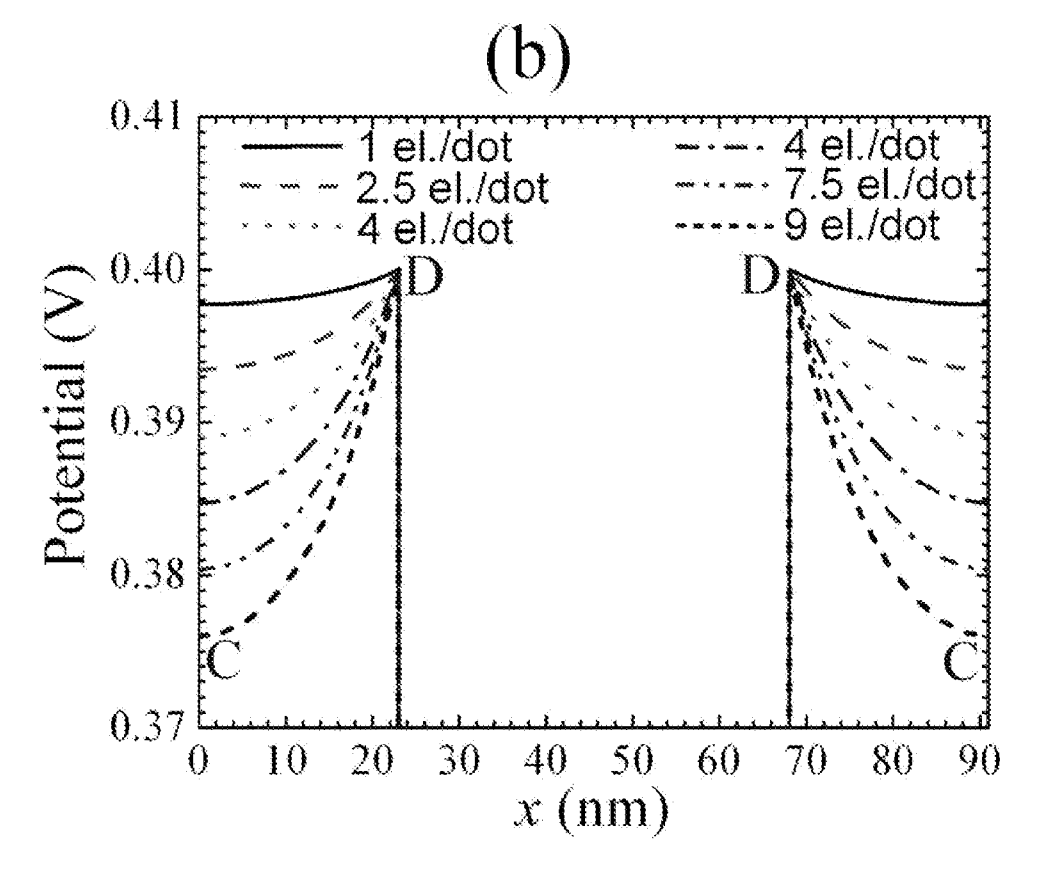


Figure 10